

PRETHERMALISATION AND THE BUILD-UP OF THE HIGGS EFFECT

D. SIXTY AND A. PATKÓS*

Department of Atomic Physics

Eötvös University

H-1117 Pázmány Péter sétány 1/A

E-mail: denes@achilles.elte.hu, patkos@ludens.elte.hu

Real time field excitations in the broken symmetry phase of the classical abelian Gauge+Higgs model are studied numerically in the unitary gauge, for systems starting from the unstable maximum of the Higgs potential.

1. Introduction

Tracking the transmutation of the angular component of a complex Higgs field into the longitudinal polarisation state of the gauge field during the termination of inflation in hybrid models might reveal interesting details of the real time Higgs effect and of the electroweak dynamics¹. The excitation rate of the different polarisation states might be different as well as the thermal relaxation rates². The production of gauged cosmic strings is another important aspect of this process³. Our numerical study concentrates on the non-equilibrium phase transition aspects.

2. Partial Pressures and Energy Densities of the Model

The main observables studied in the present investigation of the classical abelian Gauge+Higgs model,

$$L = -\frac{1}{4}F_{\mu\nu}F^{\mu\nu} + \frac{1}{2}D_\mu\Phi(D^\mu\Phi)^* - V(\Phi), \quad V(\Phi) = \frac{1}{2}m^2\Phi^2 + \frac{\lambda}{24}\Phi^4 \quad (1)$$

*Work supported by grant T-037689 of the Hungarian National Science Foundation.

are the partial energy densities and pressures:

$$\begin{aligned}
\epsilon &= \epsilon_\rho + \epsilon_T + \epsilon_L, \quad p = p_\rho + p_T + p_L, \\
\epsilon_\rho &= \frac{1}{2}\Pi_\rho^2 + \frac{1}{2}(\nabla\rho)^2 + V(\rho), \quad p_\rho = \frac{1}{2}\Pi_\rho^2 - \frac{1}{6}(\nabla\rho)^2 - V(\rho), \\
\epsilon_T &= \frac{1}{2}[\Pi_T^2 + (\nabla \times \mathbf{A}_T)^2 + e^2\rho^2\mathbf{A}_T^2], \\
p_T &= \frac{1}{6}[\Pi_T^2 + (\nabla \times \mathbf{A}_T)^2 - e^2\rho^2\mathbf{A}_T^2], \\
\epsilon_L &= \frac{1}{2}\left[\Pi_L^2 + e^2\rho^2\left(\mathbf{A}_L^2 + \frac{1}{(e^2\rho^2)^2}(\nabla\Pi_L)^2\right)\right], \\
p_L &= \frac{1}{6}[\Pi_L^2 - e^2\rho^2\mathbf{A}_L^2] + \frac{1}{2}\frac{1}{e^2\rho^2}(\nabla\Pi_L)^2.
\end{aligned} \tag{2}$$

Index T refers to the transversal, L to the longitudinal part of the gauge field \mathbf{A} . The expressions are valid in the unitary gauge: $\rho = |\Phi|$. A_0 was eliminated with the Gauss constraint. It was checked numerically that in equilibrium $\epsilon_\rho : \epsilon_L : \epsilon_T = 1 : 1 : 2$ within statistical fluctuations⁴.

The equations of motion derived from (1) were solved in the $A_0 = 0$ gauge and the solutions were transformed to the unitary gauge for measurements. Initially $\rho(\mathbf{x}, t = 0) = 0$ was put uniformly. Inhomogeneous modes beyond the region of spinodal instability (up to $|\mathbf{k}| \leq 5|m|$) were filled with low amplitude white noise. The spatial lattice spacing was chosen to $a_s = 0.35|m|^{-1}$ and the time step $\delta t = 0.04|m|^{-1}$.

3. Spectral Analysis of the Process of Excitation

Spectral representation of the energy densities $\epsilon(\mathbf{k})$ (pressures $p(\mathbf{k})$) were defined using the Fourier transform of the square root of various pieces of the local energy densities (pressures) and taking their absolute squares.

In **Fig.1** the degrees of excitation $\epsilon_T(\mathbf{k})/\epsilon_\rho(\mathbf{k})$ and $\epsilon_L(\mathbf{k})/\epsilon_\rho(\mathbf{k})$ are displayed as functions of $|\mathbf{k}|$ at different times. The low frequency part of $\epsilon_L(\mathbf{k})$ develops an over-excited peak, while $\epsilon_T(\mathbf{k})$ is excited weakly at early times. Their slow evolution towards equipartition defines an extremely long thermalisation time-scale ($\tau > 10^5|m|^{-1}$).

4. Signals for Prethermalisation

The dispersion relations $\omega^2(\mathbf{k})$ of the modes (ρ, \mathbf{A}_T) are obtained as $|\Pi_\rho(\mathbf{k})|^2/|\rho(\mathbf{k})|^2$ and $|\Pi_T(\mathbf{k})|^2/|\mathbf{A}_T(\mathbf{k})|^2$. For the longitudinal mode inspection of ϵ_L in (2) suggests $\omega_L^2(\mathbf{k}) \equiv |[e^2\rho^2\mathbf{A}_L](\mathbf{k})|^2/|\Pi_L(\mathbf{k})|^2$. The masses of

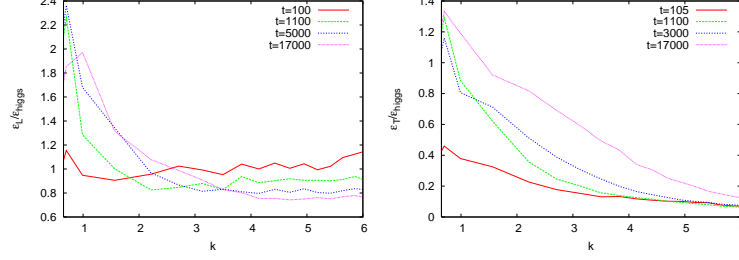


Figure 1. Evolution of the longitudinal (left) and transversal (right) energy excitations relative to the $\mathbf{k} \neq 0$ Higgs modes.

the longitudinal and transversal modes become degenerate early when calculated from modes $1 \leq |\mathbf{k}| \leq 5$; evolutionary effects are seen only at high k (see **Fig. 2**).

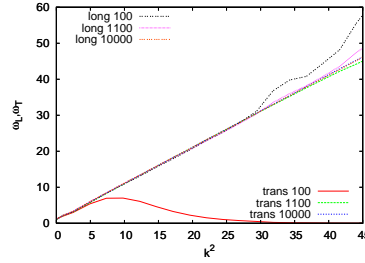


Figure 2. Evolution of the longitudinal and transversal dispersion relations

Spectral equations of state for the different fields can be defined assuming the mode-by-mode equality of the kinetic and potential spectral energy densities. Using this in (2) one arrives at the following equation for \mathbf{A}_T :

$$w_T(\mathbf{k}) \equiv p_T(\mathbf{k})/\epsilon_T(\mathbf{k}) = \mathbf{k}^2 |\mathbf{A}_T(\mathbf{k})|^2 / 3 |\Pi_T(\mathbf{k})|^2 = \mathbf{k}^2 / 3 \omega_T^2(\mathbf{k}). \quad (3)$$

Similar relation holds for ρ . Using $\omega_L^2(\mathbf{k})$ for the longitudinal mode the same formula appears on the right end of the chain if the definition $w_L(\mathbf{k}) \equiv [e^2 \rho^2 p_L](\mathbf{k}) / [e^2 \rho^2 \epsilon_L](\mathbf{k})$ is applied. The expected functional form (with newly fitted squared mass values) was compared with the measured $w_{T,L}(|\mathbf{k}|)$. The modes filled initially almost instantly obey the expected form (3). Higher $|\mathbf{k}|$ modes are gradually filled and $w(\mathbf{k})$ "climbs up" to the stable free particle behavior. These prompt features illustrate the phenomenon of "prethermalisation" ⁵ in a gauge system.

5. Gauge-Higgs Cross-Correlations

The intuitive quasi-particle picture in the unitary gauge conjectures that at low enough temperature and at moderate couplings the statistically independent field variables are just ρ , \mathbf{A}_L , \mathbf{A}_T . In the analysis of the equations of state above we avoided to rely on the statistical independence of these three variables which we are going to test next.

The transverse polarisation. The correlation coefficient between the quadratic spatial averages of ρ and \mathbf{A}_T is defined as

$$\Delta[\mathbf{A}_T, \rho] \equiv \left(\overline{\rho^2(\mathbf{x}, t) \mathbf{A}_T^2(\mathbf{x}, t)} - \overline{\rho^2(\mathbf{x}, t)} \overline{\mathbf{A}_T^2(\mathbf{x}, t)} \right) / \overline{\rho^2(\mathbf{x}, t) \mathbf{A}_T^2(\mathbf{x}, t)}. \quad (4)$$

In **Fig.3a** the time evolution of this quantity is displayed in two characteristic runs. In the first a large negative value is reached almost instantly after the Higgs-field rolls down. After a longer time interval $\Delta[\mathbf{A}_T, \rho]$ suddenly jumps to a value compatible with zero. In the other run one can observe negative "needles" occurring on the background of near-zero fluctuations.

A large negative value of the correlation coefficient (4) represents a very sensitive indicator for the presence of relativistic Abrikosov-strings. The location of the points where $\rho/|m| < 0.3$ displays a vortex network very nicely (see **Fig. 3b**), but $\Delta \approx 0$ excludes the presence of vortices.

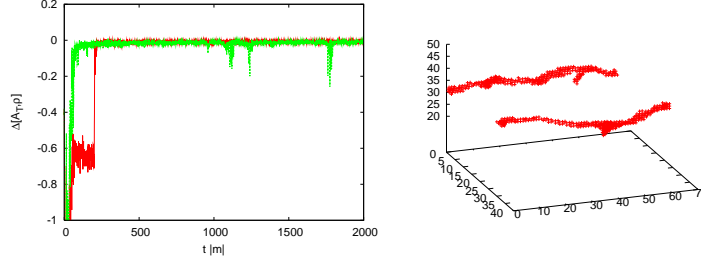


Figure 3. Non-smooth $\mathbf{A}_T - \rho$ correlation histories, and the corresponding vortex pair.

The longitudinal polarisation. The quantity $\Delta[\mathbf{A}_L, \rho]$ always displays instantly after the roll-down values significantly different from zero. and shows only a very mild time variation. It was checked that a non-zero value is present also in equilibrium⁴. This correlation coefficient linearly increases with the temperature. These observations point to the fact that the true quasiparticle field is a composite of ρ and \mathbf{A}_L . This is not a very great surprise for relatively strongly coupled systems, still it should be con-

fronted with the fact that (without vortices) $\mathbf{A}_T(\mathbf{k}, t)$ and $\rho(\mathbf{k}, t)$ perform statistically independent and Gaussian small oscillations.

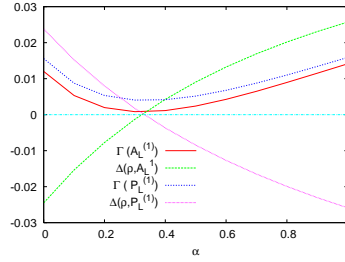


Figure 4. Correlations testing independence and Gaussianity of (5) in function of α

We have tested several trial composite fields at equilibrium ⁴. In **Fig. 4** we show the variation of $\Delta[P_L, \rho]$, $\Delta[Q_L, \rho]$ and of $\Gamma[P_L]$, $\Gamma[Q_L]$ defined by the ratio $\Gamma[Q_L] \equiv \left(\overline{(Q_L^2(\mathbf{x}, t))^2} - 3 \left(\overline{Q_L^2(\mathbf{x}, t)} \right)^2 \right) / \overline{(Q_L^2(\mathbf{x}, t))^2}$ as a function of α which characterizes the compositeness of the conjugate variables

$$Q_L(\mathbf{x}, t) = (1 + \alpha \rho^2(\mathbf{x}, t)) \mathbf{A}_L(\mathbf{x}, t), \quad P_L(\mathbf{x}, t) = \Pi_L(\mathbf{x}, t) / (1 + \alpha \rho^2(\mathbf{x}, t)). \quad (5)$$

The coefficients Γ signal deviations from Gaussianity. The nice surprise is that in equilibrium there exists a single optimal choice α_{opt} where $\Delta[P_L, \rho]$, $\Delta[Q_L, \rho]$ vanish and both Γ 's are minimal. It turns out, however, that during the non-equilibrium phase transition no such α_{opt} appears to exist, the "longitudinal quasiparticle" coordinate presumably emerges only on the thermalisation scale.

In conclusion, we found that in the abelian Higgs model an early quasi-particle characterisation works well for the dispersion relations and the equations of state just after the symmetry breaking is completed. The non-linear quasi-particle field containing the longitudinal vector component builds up much more slowly in the process of complete thermalisation.

References

1. J. Smit, Cold Electroweak Baryogenesis, to appear in Proc. of SEWM'04
2. J.-I. Skullerud, J. Smit and A. Tranberg, JHEP **0308** (2003) 045
3. M. Hindmarsh and A. Rajantie, Phys. Rev. **D64** (2001) 065016
4. D. Sexty and A. Patkós, hep-ph/0404235
5. J. Berges, Sz. Borsányi, C. Wetterich, hep-ph/0403234